Available online at www.sciencedirect.com
ScienceDirect
Journal of Power Sources 181 (2008) 353–362
JOURNAL OF POWER SOURCES
www.elsevier.com/locate/jpowsour

Environmentally friendly power sources for aerospace applications

Nieves Lapeña-Rey [a,*], Jonay Mosquera [a], Elena Bataller [a], Fortunato Ortí [a], Christopher Dudfield [b], Alessandro Orsillo [b]

[a] *Boeing Research & Technology Europe Ltd., Environmental Technologies, C/ Cañada Real de las Merinas 1-3, Building 4, 4th floor, Madrid 28042, Spain*
[b] *Intelligent Energy Ltd., The Innovation Centre, Epinal Way, Loughborough LE11 3EH, UK*

Received 25 September 2007; received in revised form 5 November 2007; accepted 7 November 2007
Available online 22 November 2007

Abstract

One of the crucial challenges of the aviation industry in upcoming years is to reduce emissions not only in the vicinity of airfields but also in cruise. Amongst other transport methods, airplanes emissions count for 3% of the CO_2 emissions. Initiatives to reduce this include not only investing in more fuel-efficient aircrafts or adapting existing ones to make them more efficient (e.g. by fitting fuel-saving winglets), but also more actively researching novel propulsion systems that incorporate environmentally friendly technologies. The Boeing Company through its European subsidiary, Boeing Research and Technology Europe (BR&TE) in collaboration with industry partners throughout Europe is working towards this goal by studying the possible application of advanced batteries and fuel-cell systems in aeronautical applications. One example is the development of a small manned two-seater prototype airplane powered only by proton exchange membrane (PEM) fuel-cell stacks, which runs on compressed hydrogen gas as fuel and pressurized air as oxidant, and Li-ion batteries. The efficient all composite motorglider is an all electric prototype airplane which does not produce any of the noxious engine exhaust by-products, such as carbon dioxide, carbon monoxide or NO*x*, that can contribute to climate change and adversely affect local air quality. Water and heat are the only exhaust products. The main objective is to demonstrate for the first time in aviation history a straight level manned flight with fuel-cells as the only power source. For this purpose, the original engine of a super Dimona HK36TTC glider from Diamond Aircraft Industries (Austria) was replaced by a hybrid power system, which feeds a brushless dc electrical motor that rotates a variable pitch propeller.

Amongst the many technical challenges encountered when developing this test platform are maintaining the weight and balance of the aircraft, designing the thermal management system and the power management between the two power sources [N. Lapeña-Rey, J. Mosquera, E. Bataller, F. Ortí, SAE 2007 Aerotech Congress & Exhibition, 2007 (Publication number: 2007-01-3906)].

The demonstrator airplane constitutes an example of the successful implementation of novel clean power sources in aviation. The detailed description of the airplane and its subsystems is given elsewhere [N. Lapeña-Rey, J. Mosquera, E. Bataller, F. Ortí, SAE 2007 Aerotech Congress & Exhibition, 2007 (Publication number: 2007-01-3906)]. This paper focuses specially on the power sources design and pre-flight tests giving special attention to those requirements derived from aerospace applications.

Keywords: Li-ion batteries; PEM fuel cells; Fuel-cell airplane

1. Introduction

Due to its very high lift to drag ratio, the power requirements of the fuel-cell demonstrator airplane are of the order of the 36 kW brake power for take-off and climb and approximately 15 kW brake power for cruise flight. The fuel-cell system is the main power source and supplies sufficient electrical power for level flight. For take-off and climb, the airplane's batteries cut in to provide the additional boost.

The main challenge encountered in the design of the airplane electrical system was the power management of these two power sources, connected in parallel, when they both provide power.

* Corresponding author. Fax: +34 91 7688408.
E-mail address: nieves.lapena@boeing.com (N. Lapeña-Rey).

0378-7753/$ – see front matter © 2007 Elsevier B.V. All rights reserved.
doi:10.1016/j.jpowsour.2007.11.045

The challenges arise because of the different electrical characteristics of both sources which means that when they are coupled in parallel in a hybrid system, the load they each deliver is not optimally balanced. In addition, the battery energy is limited, and the fuel-cell output power limitation is lower than the power requirements of the demonstrator airplane loads during the take-off and climb. The power balance was achieved by regulating the output voltage of a dc/dc converter connected in series with the fuel cell to the distribution bus (series boost converter). The output voltage of this converter sets the bus voltage, within its range of operation, thus, controlling the current sharing between the sources. Connecting the converter electrically in series, rather than in parallel, avoided processing all the fuel-cell power; thus, reducing losses and, therefore, size and weight. The regulation of the power delivered by each source was done as a function of the load to maximize the energy of the total hybrid power source. The key benefit of this approach is that it helps save the battery energy so the battery can last longer and can work at a more efficient point (lower current discharge rate), i.e., decreasing the required capacity of the battery. Therefore, in this way the size and weight of the total system was minimised to comply with one of the most stringent requirements for aeronautical application. A patent invention on the power management approach has been filed at the Spanish patent office [2].

Additional management of the power flow consists of coupling the power sources and the main load, that is, the propulsion electrical motor. This was done by commanding the propulsion motor by means of the throttle input, but also by the configuration and state of the electrical system. The throttle control avoids the steady-state propulsion motor power demand from being greater than that allocated, by reducing the motor command, when needed, to reach a balance between the electrical sources and the airplane loads. One additional functionality of the throttle control is derived by the relatively slow dynamic response of the fuel-cell system (compared to a battery); the fuel cell requires its maximum allowable rate of power change per unit time not to be exceeded. Therefore, the throttle control processes the motor request through a slew ramp limiter in order to obtain smooth power change rates.

Both the PEM fuel-cell system and the Li-ion battery used in the demonstrator airplane are thoroughly described below. Amongst the most important requirements was an acceptable specific power density for aeronautical applications, reliability and proven ability to operate in the environmental conditions expected during the flights of the demonstrator airplane, i.e., low altitude, low vibrations and tilted angles.

2. The fuel-cell system

The fuel-cell system is a pressurized system that comprises two separate proton exchange membrane stacks, electrically connected in series. The system maximum power output is approximately 20 kW net or 24 kW gross at approximately 200 V. The stacks are the cores of the fuel-cell system. The electricity is generated via an electrochemical reaction between hydrogen (H_2) and oxygen (O_2) from the air, the stacks directly converting the chemical energy into electrical energy. The stacks generate electricity continuously as long as they are supplied with the fuel and the oxidant, the reaction by-products being water and heat. When hydrogen is delivered to the stack anode, it is ionized by a catalytic reaction at the electrode, emitting electrons. The hydrogen ions pass through the electrolytic membrane (ion exchange membrane), where they react with adsorbed oxygen atoms at the cathode. An electrical potential difference exists between the anode and cathode which forces the electrons to cross from the anode to the cathode through an external circuit. Therefore, this reaction creates a direct current. Water is generated at the cathode (oxygen electrode) as a by-product and some of the product water is re-cycled for stack humidification and thermal management.

Two main requirements were taken into consideration when selecting the fuel-cell system components, i.e., safety and weight constrains. The fuel-cell system features mainly three subsystems: the air delivery, water delivery and hydrogen supply subsystem.

The air delivery subsystem supplies pressurized air, within a predetermined temperature range, to the fuel-cell stacks. A basic schematic of the air delivery subsystem is shown in Fig. 1. In the demonstrator airplane, the fuel-cell system draws air from the engine compartment through an air filter to avoid any dirt ingress. The air then flows through a mass flow meter, directly into the fuel-cell compressor, which is controlled by the fuel-cell system's main PLC controller. The air within the compressor might heat beyond 100 °C during pressurization, which in turn may compromise the performance and health of the membrane electrode assemblies (MEAs). Thus, the fuel-cell system uses an air-to-air intercooler to maintain the air inlet temperature at the fuel-cell stacks below 75 °C. The cooled air is then supplied to the cells cathode where it electrochemically reacts with the hydrogen to generate the electrical power. The un-reacted air and water exit the fuel-cell cathode and are routed through two cyclones, in order to partially recover part of the liquid water within the cathode exhaust, prior to the main condenser. The main condenser has the aim of recovering further water that is returned to the fuel cell at a later stage for cooling and humidification.

The water delivery subsystem provides water management within the fuel-cell system, supplying the required water for fuel-cell cooling, membrane humidification and re-circulating the exhaust water recovered in the fuel-cell condenser to the stacks. A basic schematic of the water delivery subsystem is shown in Fig. 1.

The water delivery system comprises two separate circuits, i.e., the water supply circuit and the water scavenge circuit. In the former the water is pumped from the two water tanks, located in the engine bay, via two water solenoid valves into the two stacks; the solenoid valves maintain equal water balances in the respective tanks. Prior to water injection into the stacks, both temperature and water flow are measured and registered. The scavenge pump re-circulates the water recovered in the condenser back into the water reservoirs. Here again the water flows through two solenoid valves to maintain the overall water balance between the respective tanks. Should the PLC controller detect different water levels in the two water reser-

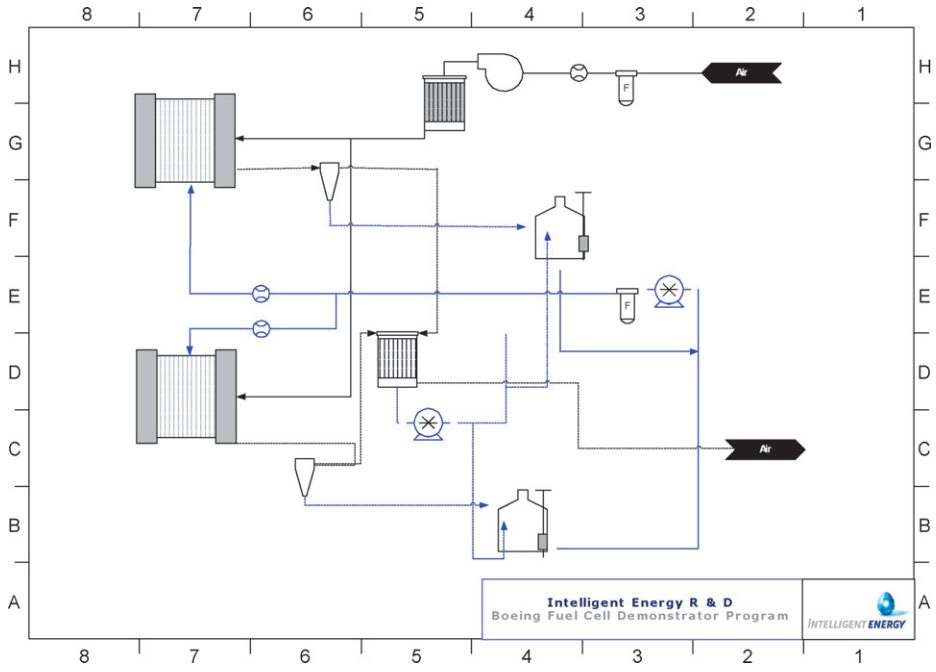

Fig. 1. Air and water delivery subsystems in the fuel-cell system of the fuel-cell demonstrator airplane.

voirs, the water solenoid valves would use water from the tank with the greater water capacity.

Finally, the hydrogen supply subsystem provides both fuel-cell stacks with hydrogen fuel at the required purity (>99.992%), operating flow and pressure during the entire flight mission. A basic schematic of the hydrogen supply subsystem is shown in Fig. 2. Driven by the need to minimise the system weight, high-pressure compressed gaseous hydrogen was chosen for this particular application. Thus, the original avgas tank of the Superdimona was substituted by a high pressure (350 bar) composite hydrogen tank, storing sufficient fuel for the entire flight mission (less than 1 h endurance). The tank is located behind the pilot's seat. The tank has an integrated solenoid valve on the neck, which includes pressure and temperature sensors, a pressure relief device and an excess flow valve. Downstream of the solenoid valve, the fuel supply subsystem includes three two-way valves in order to facilitate system operation in three different modes; external fuel supply, internal fuel supply and tank refuelling. The hydrogen pressure is reduced from the 350 bar to a medium pressure of the order of 35 bar. The medium pressure piping is sited within the cabin on the port side of the aircraft and supplies hydrogen to the engine bay, where the fuel cell is located. Within the engine bay, the hydrogen pressure is further reduced to around 3.5 bars and routed to the individual stacks. Prior to entering the stacks a third pressure regulator provides final control of the hydrogen pressure to the required level (below 1.7 bar g) for correct operation. The supply of hydrogen to the fuel-cell stacks is also controlled through an inlet solenoid valve. The system also includes two exhaust solenoid valves that control the exhaust and purge of the stacks anode.

The fuel-cell system is self-managed via an internal control unit (a PLC or programmable logic controller), which monitors the information from the internal sensors and regulates all internal actuators. The PLC performs also a regulated start-up and shut-down of the fuel-cell system. The control strategy includes an air delivery control loop, a coolant control loop, and general health monitoring and actuator control. The air delivery control loop manages the required air flow to the fuel-cell stacks, by commanding the compressor motor on the basis of the mass flow meter readings. The coolant control loop manages the required water flow for cooling and humidification purposes. In addition a number of sensors also supply information to the PLC regarding the real-time health of the fuel-cell system; should a fault be diagnosed, the PLC puts the fuel-cell system into an error state and awaits clearance by the user.

2.1. Fuel-cell tests

The fuel-cell system has been thoroughly tested against the demonstrator airplane requirements both under steady state and dynamic operating conditions. The acceptance tests were carried out with the system coupled to a programmable load unit. Steady-state testing included a conventional polarization curve and functional tests throughout the whole flight duty cycle, with the fuel cell working in a stand alone mode. In these tests the behaviour of the system was analyzed together with the parasitic losses, electrochemical hydrogen consumption and water consumption for the mission profile. The variables monitored and registered included the individual stack voltage, the current, the stack gross power, the system net power, the compressor power consumption and the 24VDC bop parasitic power, in addition to the stacks cathode inlet temperature (post-intercooler), stacks cathode exit temperature, and the cooling air flow temperature (post-condenser). The hydrogen consumption was also monitored, calculated and logged via real-time multiplication. The calculation is based on both electrochemical consumption and

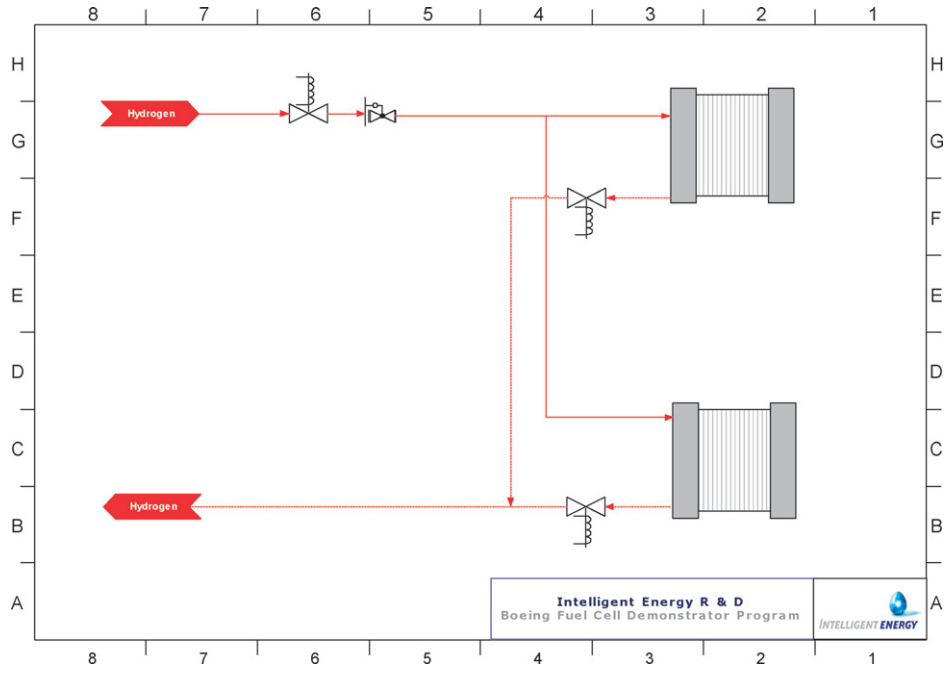

Fig. 2. Hydrogen supply subsystem in the fuel-cell system of the fuel-cell demonstrator airplane.

the anode purge losses (related to both supply pressure and purge valve control strategy).

The fuel-cell polarization curve is shown in Fig. 3 and the fuel-cell performance when subjected to the flight mission operative duty cycle is shown in Fig. 4. The fuel-cell system responded very well to the anticipated duty cycle and the compressor operated well in close loop control with the fuel cell; the system had stable operation both at its peak power output (20 kW net) and at its continuous power output (15 kW net). The PLC kept the stoichiometry constant for all flight stages. The compressor power consumption at maximum power output was around 3.24 kW whereas the ancillaries demanded approximately 130 W (Figs. 8 and 10). This is in good agreement with the results obtained for maximum power output in the polarization curve. The temperatures (stack inlet temperature, cathode exit temperatures for both stacks and the condenser exit temperatures) were maintained well below the PLC alarm trigger levels during the whole duration of the test (85 °C). In addition, the cells voltage was always above 0.4 V and the current was always well below the 150 A limit. The blower flow and pressure were always above 75 SLPM and 15 mbar g, respectively. And finally, the anode inlet pressure was always within the 700–5000 mbar g permissible range. Therefore, all variables were found to be within their acceptable limit of operation and good reproducibility was observed.

The electrochemical hydrogen consumption was calculated from the current. A total hydrogen consumption of 0.88 kg was calculated, which is in good agreement with previous experiments. The hydrogen consumption efficiency, i.e., the ratio of hydrogen consumption and the hydrogen input was above 95%.

The data from the fuel-cell polarization curve and from the flight mission helped sizing the auxiliary battery. The battery

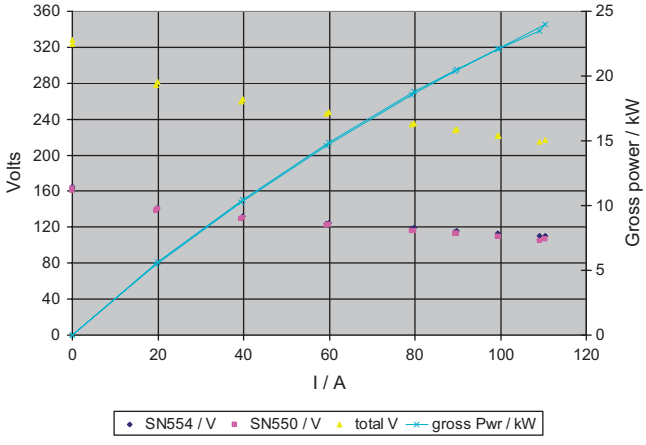

Fig. 3. Polarization curve of the fuel-cell system in the fuel-cell demonstrator airplane.

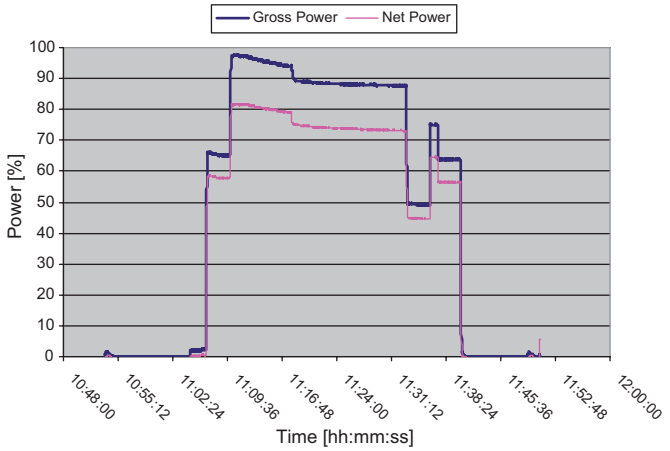

Fig. 4. Fuel-cell performance during the flight mission duty cycle of the fuel-cell demonstrator airplane.

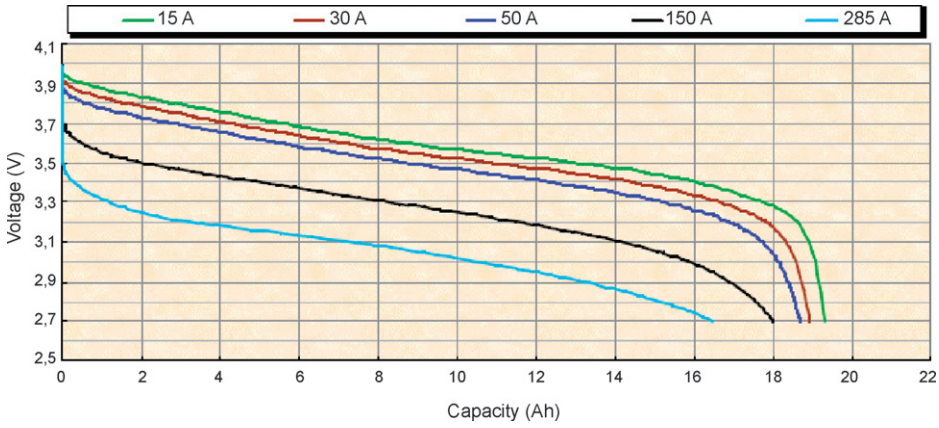

Fig. 5. Discharge curve (cell capacity and voltage as a function of current) at +20 °C of the Li-ion cells used in the auxiliary battery of the fuel-cell demonstrator airplane.

voltage range was chosen to be as close as possible to that of the fuel-cell stacks and the flight mission (take-off and climb) determined the battery capacity (Ah). This together with the Li-ion battery discharge curve, shown in Fig. 5, facilitated the design of the airplane electrical architecture as well as the power management within the power management and distribution (PMAD) box.

Performance verification tests of the system design point for continuous steady-state operation (i.e., 15 kW net) were carried out during several hours at a constant power demand to ensure that the system can maintain the required power demand without any considerable performance degradation. The fuel-cell system proved stable operation at its continuous power output for periods considerably longer than those defined for the flight mission. Moreover, the results proved to be very reproducible over a large number of runs and all parameters (including temperatures) were comfortably maintained below the PLC alarm trigger levels during the whole duration of the test. Fig. 6 shows the systems performance being stable, and without any interruption at the continuous design point (i.e., 15 kW net), for 6 h without any remarkable performance degradation. All variables were kept within the permissible limits and no alarms were triggered by the PLC. In general terms, the current fell between a range of 70 and 74 A. However, it had to be slightly adjusted (manually) towards the end of the test to maintain a constant output power. A total of 2 A were added in total within the 6-h period, which corresponds to a degradation rate of 0.33 A h^{-1}. The voltage was almost constant and always above 230 V dc. The stoichiometry was kept constant at 2.5. The compressor power consumption was around 2 kW whereas the ancillaries demanded approximately 100 W. This is in good agreement with results in previous experiments.

The objective of the performance envelope determination tests was to determine the peak power output and to determine for how long the system could operate stably under such conditions. The system was held at its maximum peak power (20 kW net) for a duration of half an hour several times, with a pause of half an hour between runs. The water reservoirs were refilled manually in the last 10 min of the tests, and were completely emptied and refilled with fresh cold deionised water between runs. The stoichiometry was kept constant at 2.5 in all cases. The results were in excellent agreement with those of the polarization curve and the duty cycle. Fig. 7 shows the maximum peak power output, 20.2 kW net, operating at approximately 107 A. All variables were found to be within their acceptable limit of operation, including inlet and cathode exit temperatures for both stacks. The system voltage was above 215 V dc. In good agreement with the values obtained during the duty cycle tests, the

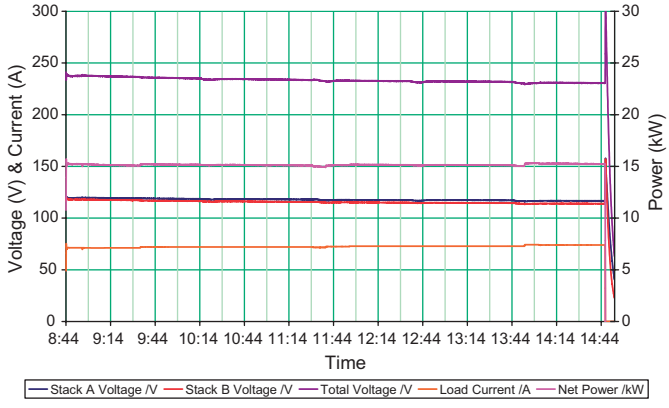

Fig. 6. Performance verification tests of the fuel-cell system in the fuel-cell demonstrator airplane (electrical data).

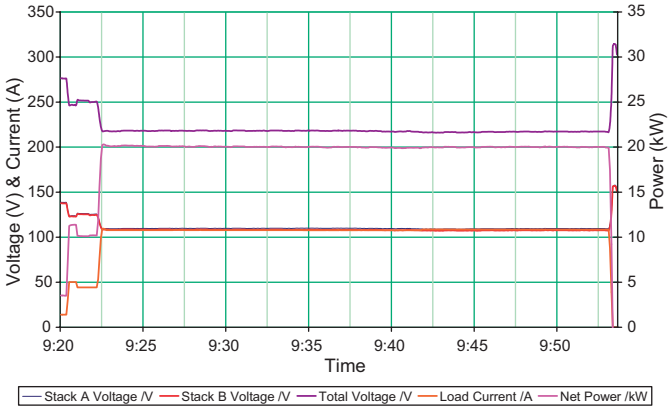

Fig. 7. Voltage, current and power data of prolonged operation at peak power output of the fuel-cell system in the fuel-cell demonstrator airplane.

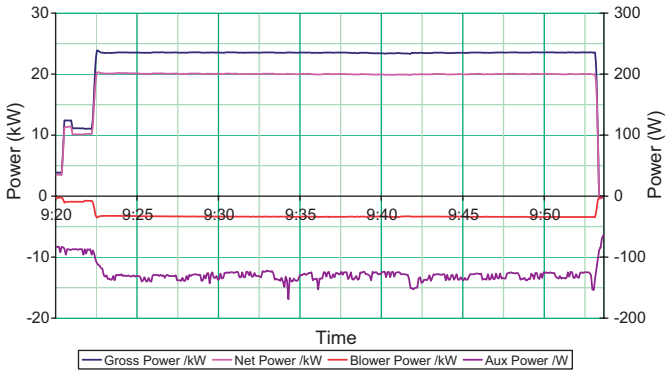

Fig. 8. Power data of prolonged operation at peak power output of the fuel-cell system in the fuel-cell demonstrator airplane.

compressor power consumption was around 3.4 kW whereas the ancillaries demanded approximately 130–140 W (Fig. 8).

The fuel-cell system dynamic testing included, small signal source impedance tests (SSSI) with ac current injected onto the dc load set-point over a range of load set-points and injection frequencies, and load transients.

The aim of the SSSI test was to characterize the behaviour of the fuel cell with ac current within the range of operating frequencies of the propulsion motor. The tests showed a substantial fuel-cell system output impedance. However, simulations show that the induced distortion could be within the operative margins; this was also demonstrated during the post-integration functional tests while powering the inverter motor of the demonstrator airplane with just the fuel-cell system. The inverter induces a current ripple that the fuel-cell delivers without any errors.

The aim of the load transient tests was to determine the fuel-cell system behaviour in non-steady-state conditions, with the compressor powered by the fuel cell, to obtain an indication of the capability of the system to cope with transients load steps that might occur during the flight. The dynamic behaviour of the system was studied and the transient response of the system with the system running automatically from the PLC was measured, monitored and registered. The natural transient response of the fuel-cell stack itself, without the PLC imposing any corrective actions, was also measured. The fuel-cell response (kW s^{-1}) is primarily determined by the lag of the compressor. The PLC response is within hundreds of milliseconds. Transient steps at low-electrical loadings are not anticipated to create any problems. However, there are concerns with large instantaneous transient steps at high-electrical loadings (from 75% to 100% load, for example). The short duration stack polarization effects result from the limiting fluid supply during the application of the transient and could possibly cause the system to enter an error mode.

The non-steady-state test results helped matching the throttle conditioning design (in the PMAD control board) to the transient response of the fuel-cell system. Moreover, in the unlikely event of a battery failure, the propulsion power demand would be reduced to the maximum fuel-cell power.

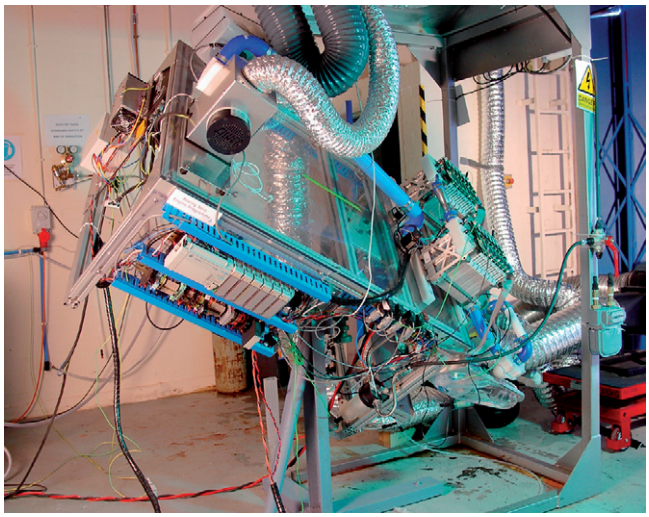

Fig. 9. Fuel-cell system in the fuel-cell demonstrator airplane during tilt testing (photo courtesy of Intelligent Energy).

Further tests included the orientation angle or tilt tests to determine the safe operating angles and acceptable orientation of the fuel-cell system components within the engine bay for sustained operation during flight (see the tilted system in Fig. 9). The performance of the system at peak power (20 kW net) was assessed at five different angles, given by their pitch and roll. The system showed no cell fluidic balance problems due to working at tilted angles (pitch plus or minus 30°, bank angle 0° or ±45°). The results are given in Fig. 10. Once again, there was good reproducibility in all tested positions and there was a close agreement with the results reported for the polarization curve and the duty cycle. The stoichiometry was kept constant at 2.5 in all cases. For test with a tilt angle of 0° roll and +30° pitch, the maximum peak power output was found to be around 20.3 kW net, operating at approximately 107 A. All variables were found to be within their acceptable limit of operation, including inlet and cathode exit temperatures for both stacks. The system voltage was above 220 V dc. The compressor power consumption at maximum power output was around 3.1 kW whereas the ancillaries demanded approximately 130–140 W.

Electrical environmental tests were also carried out by introducing voltage spikes on the dc power leads of the fuel-cell PLC.

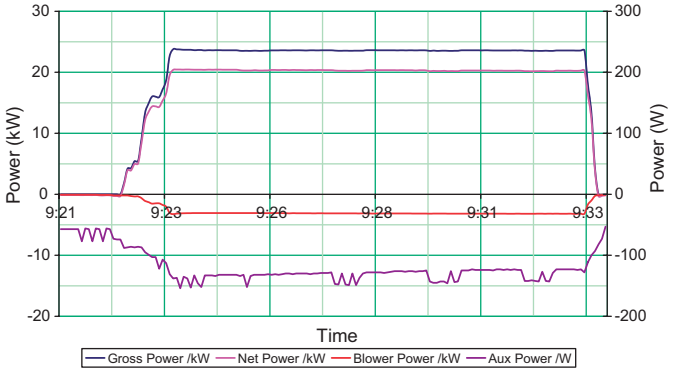

Fig. 10. Power data from orientation test at 0° roll, +30 °pitch of the fuel-cell system in the fuel-cell demonstrator airplane.

No mal-function of the fuel-cell PLC was observed. Therefore, the PLC can be regarded as immune to those transient voltage spikes.

3. The Li-ion auxiliary battery

The secondary power source in the fuel-cell demonstrator airplane hybrid power system is the auxiliary battery. Driven by the requirement of keeping the system weight as low as possible, Li-ion technology was chosen for this application. Lithium-ion batteries are a type of rechargeable battery of common use in the consumer electronics. Their most important advantage is the energy-to-weight ratio and the slow loss of charge when inoperative compared with other battery technologies. A further strength of the Li-ion chemistry resides in the high open circuit voltage per cell when compared with other battery technologies, typically from 3.3–4.0 V cell^{-1}.

The auxiliary battery is made of several high-power cells electrically connected in series and arranged in modules. The cell technology and the number of cells were determined from the results of simulations of the electrical performance of the entire system to match the energy demands and voltage range. The demonstrator battery has an internal management unit, which controls the first level system cell management and contains the centralized electronic system to manage the battery, the charge, discharge and state of charge algorithms. The battery also includes different sensors, a contactor and a fuse designed for battery protection in case of battery over-voltage, over-current in both directions, over-temperature and deep discharge.

The batteries have been sized taking into account the EASA CS-22 sailplanes and powered sailplanes [3] minimum rate of climb requirement (ROC > 1.5). The batteries are only used as auxiliary power for this initial phase but have enough residual energy to be able to power the approach and land of the aircraft in case of emergency if desired.

The cells, the battery management unit and all required protections and sensors are contained within an aluminium battery case that has no cooling requirements. The case was designed to be compliant with the loads given in the EASA CS 22 aeronautical standard [3]. This implies that the case withstands 9 g forward (along the flight direction), 4.5 g upward and downward, and 3 g sideward. In case of a crash landing the battery case might be deformed or deteriorated but is robust enough to maintain the pilot safety by being self-contained. Since the battery case must withstand cell burst without any expelled gases or electrolyte vented off board, there is a single stainless steel vent port at the battery back. This port has been piped to the aircraft exterior.

3.1. Li-ion battery tests

The Li-ion battery was extensively tested against the fuel-cell demonstrator airplane requirements. During static discharges at constant current, the battery was tested according to the discharge profiles expected during the flight mission. The objective of the tests was to assess the voltage ranges, the battery capacity and the longest possible duration of the discharges before reaching its minimum acceptable voltage. The discharges were done at 20 and 10 °C to check possible cooling issues, the later being the most probable temperature at which the airplane will fly, due to the thermal management limitations imposed by the motor and the fuel-cell system radiators being in series and sharing the cooling air flow through the engine bay.

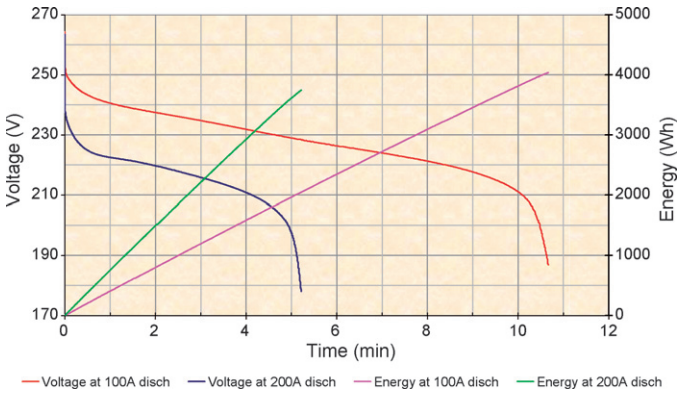

Fig. 11. Fuel-cell demonstrator auxiliary battery discharge at +10 °C during take-off & climb in normal (100 A) and emergency (200 A) operation.

In a first test, the battery discharge current was that expected during the take-off and climb when the battery is working in parallel with the fuel cell (100 A). During at least 7 min the battery is discharging at a constant current. In a second test, the battery discharge simulated the total power requirements resulting from a possible fuel cell failure during take-off and climb, i.e., 200 A. The assessment of the duration of the discharge at this abnormally high current was crucial to have an indication of the time that the pilot would have to get up to a safe altitude to perform an emergency landing should the fuel cell fail during take-off and climb. In both tests the parameters were always within the operative limits and thus the battery protections did not attempt to disconnect it. The cell temperatures were well below the limit in all cases, even during the discharge at 200 A at 20 °C.

The results are shown in Fig. 11. The battery has to provide approximately 25 kW during the 7 min take-off and climb. However, it is able to deliver a maximum continuous power in the range of 50–75 kW for a shorter time. Should the fuel cell fail during the take-off and climb the battery is able to provide enough power to get the airplane up to a safe enough altitude for the pilot to proceed with an emergency landing.

At its normal operating conditions the battery lasts over 10 min before it reaches the minimum acceptable voltage. This occurs both at 20 and 10 °C. In fact, the results were better than those expected when estimating the battery performance from single cell results. This is due to a slight increase in cell temperature when the battery is assembled, resulting in a slight decrease of the battery internal resistance and thus slightly improving the battery performance. If fully charged, the battery would only last 4.5 min at 10 °C and 5 min at 20 °C when discharging at double the normal operative current. This would guarantee a safe altitude for the flight (approximately over 300 m). This would be the worst case scenario.

The dynamic test simulated as much as possible the transient that the battery would suffer should there be a fuel cell failure

during take-off and climb. The objective of the test was to make sure that the failure of the fuel cell does not imply a failure of the battery. The tests were performed at 10 °C simulating the operating temperature of the aircraft, the worst case scenario for the battery performance.

The battery showed a good capability to cope with the imposed transient keeping all parameters well within the battery operative limits. The results indicated that the transient imposed to the battery in the event of a fuel cell failure during take-off would not disconnect the battery or damage its cells but there was an average voltage drop of approximately 10 V per step.

The Li-ion battery has to be recharged before each flight mission that the glider performs. This will be done on the ground and the battery charger will be part of the ground support equipment. Overcharging or heating above 100 °C could result in thermal runaway of both electrodes leading to generation of several gases. This could be dangerous if the cell vent failed to operate correctly. In the best case scenario, overcharging reduces the activity of the active materials in the electrodes reducing the cells life. Therefore, the charging conditions need to be extremely carefully controlled even if the battery controls protect from over-voltage, over-current, over-temperature and short-circuit events. The charge consists in a constant current/constant voltage profile. The constant current phase is applied until the battery voltage reaches its maximum permissible value. The charging current (I_c) during the constant current phase depends on the battery temperature. Then, the charger maintains the battery at this voltage by decreasing the current until the battery is fully charged. However, the charger remains connected in float mode with a current limitation in order to maintain the battery voltage below its maximum permissible value. The total charging time is approximately 3 h.

4. Pre-flight analysis: airplane post-integration functional bench tests

Following the individual component testing and the subsystems on-board installation, the entire system was thoroughly tested in the bench test configuration at the post-integration functional tests (PIFT). The main objective of the PIFT campaign was to determine the systems acceptance prior to any ground and flight tests.

Within the PIFT tests, the complete aircraft excluding the propeller and on-board hydrogen storage system was tested. The propeller was replaced by a custom-designed hydraulic brake capable of handling up to 40–45 kW (maximum estimated motor input power during take-off and climb around 41 kW) and directly coupled to the electric motor. Apart from this, for the first PIFT stages an external power supply was required to simulate the fuel cell, for the fuel cell start up and in order to simulate the auxiliary battery. To simulate the cooling air flowing through the engine bay, a vacuum fan was used and ducted together with the airplane cowling flap. Finally, the hydrogen fuel and the nitrogen for fuel-cell purging were supplied from an external source rather than from the aircraft on-board fuel system.

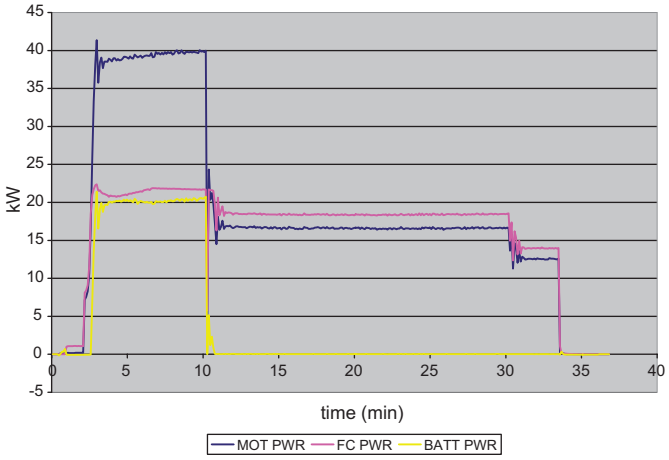

Fig. 12. Fuel-cell demonstrator motor behaviour during the simulated flight mission at the airplane bench tests.

The main electrical configurations tested during the PIFT tests in order to progressively verify the correct operation of all on-board subsystems were:

- External power supply connected to the HV bus.
- External power supply connected to the battery input terminal.
- Battery connected to the battery input terminal.
- Battery connected to the battery input terminal + external power supply connected to fuel-cell terminal.
- External power supply connected to the battery input terminal + fuel cell connected to fuel-cell terminal.
- Battery connected to the battery input terminal + fuel cell connected to fuel-cell terminal.

The correct operation of the electrical system, fuel-cell system, auxiliary batteries, control system and instrumentation system was thoroughly checked. The electrical parameters, system temperatures, power management, energy availability and hydrogen consumption were measured and analyzed.

The different tests concentrated mainly on the following:

- Correct implementation of subsystems (fuel cell, battery and electric motor)

  Paying special attention to: (i) the correct operation of the series boost converter; the SBC increases the power delivered by the fuel cell in detriment of the battery power, and makes the fuel cell work at full power during take-off and climb; (ii) the throttle limitation, which controls the motor torque command, taking into consideration the available power in the sources, and limits the torque demand ramp.
- Electrical protections operation

  Together with contactor controls when the PMAD detects and anomalous operation.
- Response to electrical transients

  Focussing specially on the response to a possible source trip-off. The disconnection of the fuel cell when both sources are working at full power (take-off and climb) causes a transient that the battery withstands without any problems. After

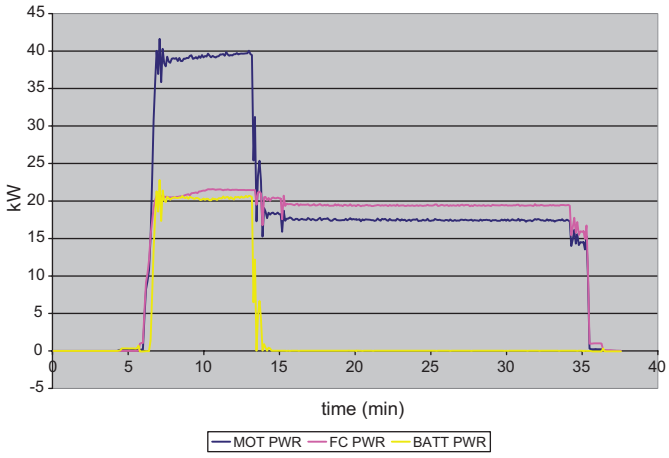

Fig. 13. Electrical powers registered during the simulated flight mission at the airplane bench tests.

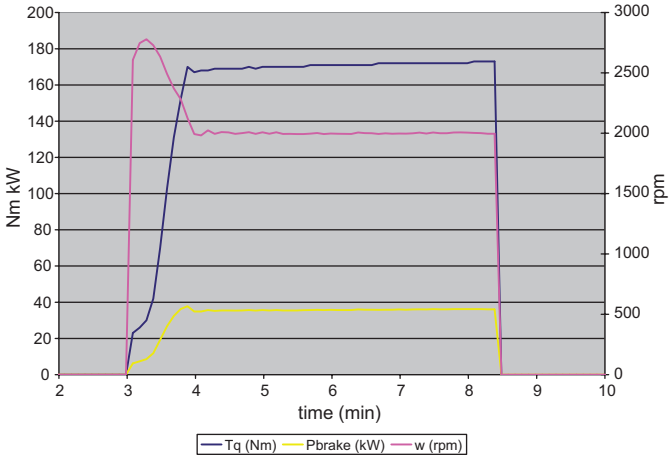

Fig. 14. Fuel-cell demonstrator airplane motor behaviour during a simulated emergency take-off mission (motor powered just by the battery) at the airplane bench tests.

the disconnection, the battery delivers all the power. However, a disconnection of the battery would cause the fuel cell to trip-off, leading to a total power loss.

- Simulation of flight profile

  As shown in Fig. 12, the final mission testing consisted on a 7–9 min take-off and climb with a maximum take-off power of 35 to 36 kW brake power and a 15–20 min cruise at around 15–16 kW brake power.

During these stages special attention was given to the motor and electronics temperatures. Regarding the motor, all temperatures remained well below the thermal limits during the entire mission with maximum temperatures in the inverter reaching 42 °C and in the motor being below 100 °C. This verified the assumptions taken to design the motor radiator. In terms of the PMAD electronics, the temperatures were also below the 100 °C limit; the maximum temperatures correspond to the power converters and the power diodes. During the tests, the maximum value (82 °C) was registered at the converters of the SBC at the end of the take-off and climb.

Regarding the recorded speeds, it must be noted that the speed fluctuations of around 500 rpm especially during the mission start and during the speed change between take-off and cruised were caused by the extremely low-hydraulic brake inertia. These speed transitions will be further analyzed with the propeller during the airplane ground tests.

Regarding the implementation of the different power sources, Fig. 13 shows the power contribution of each of the power sources. During the take-off and climb phase the Li-ion battery provides around 20 kW, half of the overall power. When the airplane reaches the cruise altitude, the battery is then disconnected and the fuel-cell system provides all the power required for cruise.

The response of the hybrid system to emergency situations (i.e., loss of one of the power sources) was also tested (Figs. 14 and 15). In order to test a possible loss of the fuel cell during the take-off after there is no possibility of aborting it, battery discharges were performed to assess the maximum battery duration and check the viability of completing an emergency take-off and climb with the battery as the only source of power.

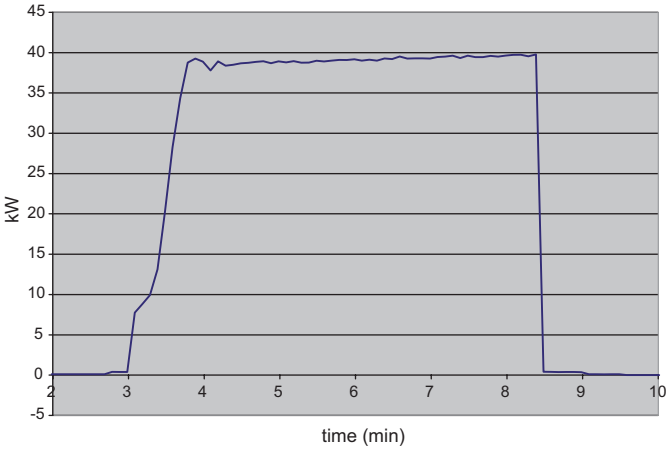

Fig. 15. Fuel-cell demonstrator airplane auxiliary battery power during a simulated emergency take-off mission (motor powered just by the battery) at the airplane bench tests.

The discharges were performed at different ambient temperature rating from 18 °C to around 26 °C. The average discharge duration was of the order of 5 to 5 and a half minute (Fig. 15). During this time the battery provides the entire power required to take-off and climb to around 300 m to a 180° turn and land safely.

5. Conclusion

The demonstrator airplane constitutes an example of the successful implementation of novel environmentally friendly power sources in aviation. The prototype aircraft comprises a PEM fuel cell and a Li-ion battery driving an electric motor coupled to a propeller. Apart from the mechanical integration challenges, i.e., integration of all subsystems in a reduced volume and maintaining the weight and balance of the aircraft, and thermal management, which are explained in detail elsewhere [1], the main electrical integration challenge was the power management of the two power sources during take-off. This was successfully achieved by regulating the output voltage of a dc/dc

converter connected in series with the fuel cell to the distribution bus (series boost converter). Connecting the converter electrically in series with the fuel cell optimized the system size and weight. In addition, the throttle control avoids the steady-state propulsion motor power demand from being higher than the allocated by the sources by reducing the motor command, when needed, to reach a balance between the electrical sources and the airplane loads. The throttle control also processes the motor request through a slew ramp limiter in order to obtain smooth power change rates to match the dynamic response of the fuel-cell system.

Both power sources were thoroughly tested to prove compliance with the airplane requirements. The fuel cell was subjected to steady-state testing comprising a polarization curve and a duty cycle, as well as to dynamic testing (ac impedance and transient test). Both the continuous and the peak power output were verified and the power and fluids consumption were verified for the anticipated flight mission. Tilted tests were also successfully accomplished. The Li-ion battery was subjected to steady-state discharges at those currents expected for take-off (for normal and failure operative modes), as well as to transients tests, to verify that the disconnection of the fuel cell for cruise would not trip the battery off.

The correct operation of the entire system was thoroughly checked during the airplane bench tests. The correct operation of the series boost converter, balancing the power delivered by each power source and making the fuel cell work at full power during take-off and climb was verified along with the throttle limitation. The response of the system to electrical transients was also monitored paying special attention to a possible source trip off. Regarding the simulated flight mission in the bench, both the motor temperatures and the PMAD electronics temperatures remained below the thermal limits during the entire mission. In the event of a fuel cell failure during take-off and climb, the battery proved to provide the entire power required to take-off and climb to approximately 300 m, an altitude safe enough for the pilot to perform a 180° turn and land safely.

Summarizing, the airplane pre-flight evaluation at the bench tests has been successfully completed and the system has worked as expected. Remaining work for the ground tests includes testing the proper operation of the propeller (absence of vibrations, speed and pitch control), testing the propeller adapter, verifying the cooling assumptions and the ventilation through the engine bay, and testing the effect of vibrations on the fuel-cell, fuel system, PMAD electronics and external connections. The ground tests are on-going and the results will be published promptly.

Acknowledgments

The Boeing Research & Technology, Europe (BR&TE) team members would like to express their most sincere gratitude to the entire industry team that has helped Boeing to develop and test the fuel-cell-demonstrator airplane. BR&TE has worked closely with its colleagues in Phantom Works and Boeing Commercial Airplanes, its Spanish partners, and with companies in Austria, France, Germany, the United Kingdom, and the United States, to design and assemble the experimental Boeing fuel-cell demonstrator airplane.

The fuel-cell system used on the flight demonstrator, for instance, was designed and built by the UK-based company Intelligent Energy. The airplane itself is a Dimona motor glider, built by Diamond Aircraft Industries of Austria. The Madrid-based avionics group Aerlyper performed airframe modifications, as well as mounting the wiring of all components; SAFT France designed and assembled the Li-ion auxiliary battery and backup Ni/Cd battery; Air Liquide Spain performed the detailed design and assembly of the on-board fuel system and the refuelling station; the Centre of Industrial Electronics of the Polytechnic University of Madrid (School of Industrial Engineering) collaborated in the design and construction of the power management and distribution box; post-integration bench testing is being conducted in a facility that belongs to the Polytechnic University of Madrid; and SENASA (Spain) will provide a test pilot and facilities for flight tests. Other suppliers include UQM Technologies Inc. (United States) manufacturers of the UQM Power Phase 75 electric motor, MT Propeller (Germany) manufacturers of the MTV-1-A/175-05 variable pitch propeller, Técnicas Aeronaúticas de Madrid (Spain) manufacturers of the propeller adapter, Ingeniería de Instrumentación y Control (Spain) manufacturers of the motor radiator, GORE (Germany) providers of the Membrane Electrode Assemblies (MEAs) for the fuel-cell system, Indra (Spain) and Inventia (Spain). Tecnobit in Spain has thoroughly helped the BR&TE test team at the airplane bench and ground tests.

References

[1] N. Lapeña-Rey, J. Mosquera, E. Bataller, F. Ortí, Proceedings of the SAE 2007 Aerotech Congress & Exhibition, 2007 (Publication number: 2007-01-3906).

[2] E. Bataller, J. Oliver, O. García, Invention disclosure F710000006, Energy optimization of a fuel-cell/battery hybrid power sourcefiled in Q1, 2007.

[3] EASA CS 22 Aeronautical Standard.